Toxicology in Vitro 60 (2019) 281–292

Contents lists available at ScienceDirect

Toxicology in Vitro

journal homepage: www.elsevier.com/locate/toxinvit

Protein pathway analysis to study development-dependent effects of acute and repeated trimethyltin (TMT) treatments in 3D rat brain cell cultures

Domitille Schvartz[a,b], Víctor González-Ruiz[b,c], Nadia Walter[a,b], Paola Antinori[b,d], Fabienne Jeanneret[b,c], David Tonoli[b,c], Julien Boccard[b,c], Marie-Gabrielle Zurich[b,e], Serge Rudaz[b,c], Florianne Monnet-Tschudi[b,e], Jenny Sandström[b,e,1], Jean-Charles Sanchez[a,b,*,1]

[a] Translational Biomarker Group, Department of Internal Medicine Specialties, University of Geneva, Geneva, Switzerland
[b] Swiss Centre for Applied Human Toxicology (SCAHT), Switzerland
[c] Analytical Sciences, School of Pharmaceutical Sciences, Universities of Geneva and Lausanne, Geneva, Switzerland
[d] Neuroproteomics group, Department of Clinical Neurosciences, University of Geneva, Geneva, Switzerland
[e] Department of Physiology, University of Lausanne, Lausanne, Switzerland

A B S T R A C T

Trimethyltin is an organometallic compound, described to be neurotoxic and to trigger neuroinflammation and oxidative stress. Previous studies associated TMT with the perturbation of mitochondrial function, or neurotransmission. However, the mechanisms of toxicity may differ depending on the duration of exposure and on the stage of maturation of brain cells. This study aim at elucidating whether the toxicity pathways triggered by a known neurotoxicant (TMT) differs depending on cell maturation stage or duration of exposure. To this end omics profiling of immature and differentiated 3D rat brain cell cultures exposed for 24 h or 10 days (10-d) to 0.5 and 1 μM of TMT was performed to better understand the underlying mechanisms of TMT associated toxicity.

Proteomics identified 55 and 17 proteins affected by acute TMT treatment in immature and differentiated cultures respectively, while 10-day treatment altered 96 proteins in immature cultures *versus* 353 in differentiated. The results suggest different sensitivity to TMT depending on treatment duration and cell maturation. In accordance with known TMT mechanisms oxidative stress and neuroinflammation was observed after 10-d treatment at both maturation stages, whereas the neuroinflammatory process was more prominent in differentiated cultures than in the immature, no development-dependent difference could be detected for oxidative stress or synaptic neurodegeneration. Pathway analysis revealed that both vesicular trafficking and the synaptic machinery were strongly affected by 10-d TMT treatment in both maturation stages, as was GABAergic and glutamatergic neurotransmission.

This study shows that omics approaches combined with pathway analysis constitutes an improved tool-set in elucidating toxicity mechanisms.

1. Introduction

It is generally accepted that the developing brain exhibits higher sensitivity to toxicant-exposure than the adult brain (Aschner et al., 2017; Bal-Price et al., 2015; Grandjean and Landrigan, 2014). Therefore, there is a particular interest in understanding the underlying mechanisms leading to neurotoxicity and whether these differ depending on the state of brain cell maturation. The neurotoxicant trimethyltin (TMT) is widely used as a plastic stabilizer and as a biocide, and has been detected in both drinking water supplies and in marine environments (Shin et al., 2016). *In vivo* studies have shown that TMT is highly neurotoxic, with a particular selectivity for hippocampus in the limbic system (Corvino et al., 2013; Little et al., 2012), and observation *in vitro* show that the brain cell maturation stage influence its susceptibility to TMT treatments (Hogberg et al., 2009; Monnet-Tschudi et al., 1995a; Sandstrom et al., 2017). TMT-induced neurotoxic mechanisms include excitotoxicity, calcium homeostasis disruption, mitochondrial dysfunction, oxidative stress, disruption of glutathione metabolism, and neuroinflammation (Grandjean and Landrigan, 2014; Shin et al., 2016; Corvino et al., 2013; Little et al., 2012; Geloso et al., 2011; Lee et al., 2016; McCann et al., 1996). Although glutamate excitotoxicity is well described in these models, TMT effect on neurotransmission of GABAergic neurons (Andersson et al., 1995; Brambilla et al., 2003; Kim et al., 2015; Wong et al., 2003) seems to be more variable. TMT intoxication is followed by seizures, behavioural alterations and cognitive deficits (Corvino et al., 2013; Geloso et al., 2011) and acute poisoning causes similar symptoms in humans (Yoo et al., 2007). However, the effects on human health due to exposure to tin compounds found in the environment is not known (Agency for Toxic Substances and Disease Registry (ATSDR), 2005).

TMT-induced neurotoxicity is also accompanied by the induction of neuroinflammation. Microglial activation and the release of

* Corresponding author at: Translational Biomarker Group, Department of Internal Medicine Specialties, University of Geneva, Geneva, Switzerland.
E-mail address: Jean-Charles.Sanchez@unige.ch (J.-C. Sanchez).
[1] Contributed equally.

https://doi.org/10.1016/j.tiv.2019.05.020
Received 14 December 2018; Received in revised form 18 March 2019; Accepted 29 May 2019
Available online 07 June 2019
0887-2333/

inflammatory cytokines (Kim et al., 2014) and mediators of inflammation (IL-1ß, TNF-α and IL-6) were observed upon TMT exposure in various models (Kim et al., 2014; Bruccoleri et al., 1998; Fiedorowicz et al., 2001; Harry et al., 2008; Harry and Lefebvre d'Hellencourt, 2003; Harry et al., 2002; Little et al., 2002). These processes are followed by astrocyte activation, evidenced mainly by morphological changes and by increased expression of the specific marker glial fibrillary acidic protein (GFAP) (McCann et al., 1996; Kim et al., 2014; Teismann and Schulz, 2004).

Omic-profiling-strategies combined with pathway analysis have proven to be powerful tools for revealing complex biological processes (Nemes et al., 2013; Wilmes et al., 2013) and such approaches have already successfully been used in several *in vitro* models of neurotoxicity (Wilmes et al., 2013; van Vliet et al., 2008; Schultz et al., 2015; Pottiez et al., 2011). These holistic and untargeted approaches can contribute in identifying specific molecular pathways as well as the cellular phenotypic adaptations triggered upon toxicant exposure (Nicholson et al., 2002; Nicholson et al., 1999).

In this study we aimed at investigating whether these approaches can be used to detect differences in TMT-elicited toxicity pathways depending on brain cell maturation stage and exposure duration. To this end we used *in vitro* 3D cultures of rat brain cells, a culture system – comprising different neuronal subtypes as well as oligo-, astro- and microglial cells - that undergoes differentiation during the culture period, including synaptogenesis and myelination, reaching a high degree of differentiation with the establishment of mature synapses and compact myelin (Zurich et al., 2003). This culture system has been widely used for neurotoxicity studies and has allowed the detection of development-dependent neurotoxicity of lead and mercury (Zurich et al., 2002; Monnet-Tschudi et al., 1996), which are known developmental neurotoxicants (Aschner et al., 2017; Grandjean and Landrigan, 2014). The high yield and reproducibility of the cultures enable multiparametric endpoints analysis, including “omics” approaches (Schultz et al., 2015).

Based on the assumptions that not only the maturation state of the brain cells but also the duration of the exposure may trigger different effects and/or different toxicity pathways, 3D rat brain cell cultures were exposed to TMT at two different maturation stages, either acutely (for 24 h) or repeatedly (for 10 days). Using proteomics and pathway enrichment analysis, we aimed to define specific signatures of acute *versus* repeated exposure to TMT, as well as investigating toxicity response, pathway differences and similarities in relation to the brain cells' maturation stages.

2. Experimental procedures

2.1. 3D rat brain cell culture

Serum-free 3D brain cell cultures were prepared from the whole brain of 16-day embryonic rats (Sprague Dawley, Janvier, France) as previously described (Honegger et al., 2011). In short, a culture batch, considered as an independent experiment, was prepared with the whole brain of approximately 70 pups obtained from 6 different pregnant rat dams. Each culture flask received 10 million living cells at culture initiation. Cultures were maintained in a chemically defined medium under constant gyratory agitation (80 rpm) at 37 °C in an atmosphere of 10% CO_2 and 90% humidified air, allowing the rapid formation of about 1200 3D structures (free-floating spheres) per original flask. Media were freshly replenished every third day until day *in vitro* (DIV) 14, and every second day thereafter. During the culturing period, post-mitotic neurons undergo progressive differentiation, while glial cells precursors still proliferate during the first two weeks in culture and differentiate thereafter, reaching a high degree of differentiation with the presence of compact myelin. Replicate cultures, containing an average of 150–200 free-floating spheres, were prepared by pooling and redistributing the free-floating spheres of several original culture flasks (Honegger et al., 2011; Honegger et al., 1979). Two to three replicate cultures per treatment were used in each independent experiment.

2.2. Trimethyltin chloride treatments

Trimethyltin chloride (TMT) (Sigma-Aldrich, CAS Number: 1066-45-1, PubChem Substance ID: 24848783) was diluted in ultrapure water to prepare 100-fold stock solutions of 50 and 100 µM concentrations. For exposure of the cell cultures, aliquots of the stock solutions were added directly to the culture medium to reach nominal culture media concentrations of 0.5 and 1.0 µM TMT. At each culture media change (2.5 mL out of 4 mL), TMT was added to maintain a constant nominal concentration in the culture media. Cultures were exposed at an immature stage, beginning at day *in vitro* (DIV) 5, and at a highly differentiated (mature) stage beginning at DIV 25. Cultures were harvested either 24 h after the first exposure (acute treatment) or at the end of the 10-day repeated exposure, hence at DIV15 or at DIV35, respectively.

2.3. Protein content and Lactate Dehydrogenase (LDH) activity measurements

3D cultures were washed in PBS and homogenized by sonication in 400 µL of 2 mM potassium phosphate buffer containing 1 mM EDTA, pH 6.8. Homogenates were divided in aliquots for determination of total protein content by the Lowry method (Honegger et al., 1979). Intracellular lactate dehydrogenase activity (LDH, EC 1.1.1.27) was measured in the cell homogenates by conventional photometric assay as described by Koh and Choi (Lowry et al., 1951; Koh and Choi, 1987). LDH catalyses the transformation of pyruvate into lactacte in presence of NADH, which is oxidized. The velocity of NADH decrease measured by photometry (absorbance measured at 340 nm) is directly proportional to intracellular LDH activity measured in homogenates. The values of LDH activity found in the cell homogenates of the untreated controls represent 100% of living cells, and are set at 1.

2.4. Western blots

Three-dimensional cultures were washed twice with PBS at 4 °C and homogenized in RIPA (Millipore) with protease inhibitors (Complete, Roche). The protein content of the homogenates was measured with BCA assay. NuPage LDS Sample Buffer (Invitrogen) and NuPage Sample Reducing agent (Invitrogen) were added to the samples and the mixtures heated at 99 °C for 5 min.20 µg of protein was loaded per well. Proteins were separated using NuPage 12% Bis-Tris gels (Invitrogen) and MOPS running buffer (Invitrogen) at a constant voltage (100 V, 1 h30). Proteins were transferred to nitrocellulose membranes (BioRad) for 7 min at a constant voltage (25 V) under semi-dry condition (Transblot SD semi-dry transfer cell, BioRad) using Towbin transfer buffer (25 mM Tris base, 192 mM glycine, and 20% methanol). Membranes were blocked with 5% non-fat dry milk in TBS-Tween (20 mM Trizma base, 137 mM NaCl, 0.05% Tween, pH 7.6). After blocking, membranes were incubated overnight at 4 °C with anti-synaptotagmin-1 antibody (Abcam, 2 µg/mL) diluted in 5% non-fat dry milk and TBS. The membranes were then washed with TBS and labeled with horseradish peroxidase conjugated rabbit anti-goat IgG (1:10000, Biorad). A second wash was performed and blots were visualized by chemiluminescence (ECL, Amersham). The resulting bands were scanned and band intensity was quantified with image analysis (Image J). Data were acquired in arbitrary densitometric units and transformed to percentages of densitometric levels obtained from scans of control samples visualized on the same blot.

2.5. Gene expression analysis by quantitative real-time PCR

Total mRNA was prepared with the RNeasy kit (Qiagen,

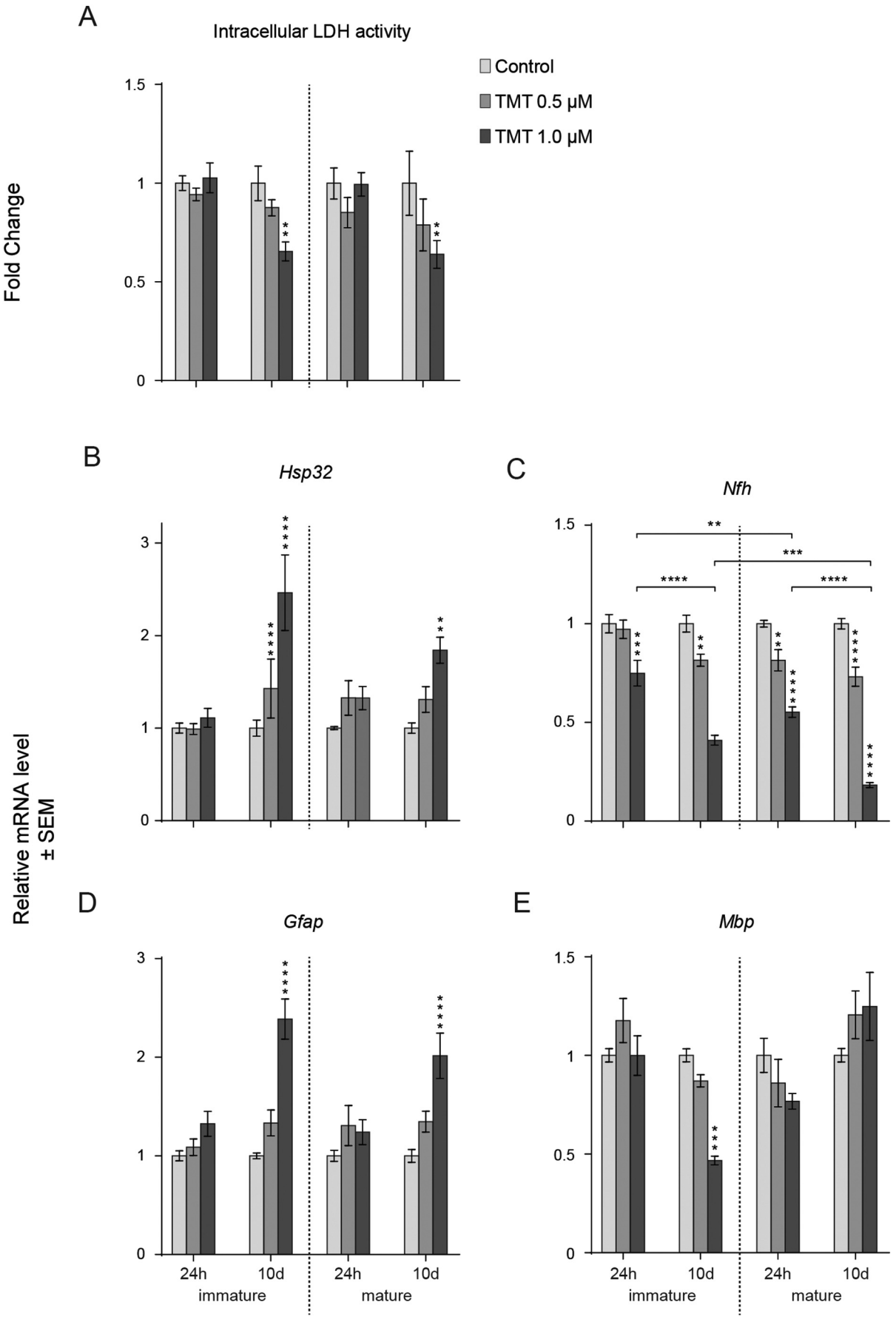

(caption on next page)

Fig. 1. Neurotoxicity assessment for immature and mature rat brain cell cultures submitted to acute (24 h) and prolonged (10d) TMT treatments. A/TMT effect on lactate dehydrogenase (LDH) activity. B/TMT effects on the mRNA expression of *Hsp32*, a marker of oxidative stress. C/TMT effects on the mRNA expression of *Nfh*, a marker of neurons. D/TMT effects on the mRNA expression of *Gfap*, a marker of astrocytes E/TMT effects on the mRNA expression of *Mbp*, a marker of oligodendrocytes.
Data represents the mean of 5–6 replicates obtained in 2–3 independent experiments. Bars correspond to the standard error of the mean (SEM). Statistical significance of each measure from treated cells toward the control culture is evaluated with a 2-ways ANOVA test in conjunction with Tukey's multiple comparison test. Significant *p*-values: * < 0.05; ** < 0.01; *** < 0.005; **** < 0.001.

Switzerland) according to manufacturer's guidance and yield was determined by spectrophotometry (NanoDrop, ND-1000). Reverse transcription was performed on 1 microgram total RNA with the High Capacity cDNA Reverse Transcription kit (Life Technologies, US). Real-time PCR analyses were performed using Power SYBR Green (Life Technologies, USA) and 3.2 ng of cDNA per reaction for detection of *Nefh* (fw 5′-caggacctgctcaacgtcaa-3′, rev 5′-cttcgccttccaggagttttct-3′), *Gfap* (fw 5′-ccttgacctgcgaccttgag-3′, rev 5′-gcgcatttgcctctcacacaga-3′), *Mbp* (fw 5′-gcacgctttccaaaatctttaag-3′, rev 5′ agggaggctctcagcgtctt-3′), *Hsp32* (fw 5′-agg tgt cca ggg aag gct tt-3′, rev 5′- tcc agg gcc gta tag ata tgg t-3′). All primers were examined for potential off-targets, validation of amplification of amplicon of correct size also at high cycle numbers (> 40), as well as passing validation for efficacy (for ΔΔCt method) prior to usage. Beta-actin (*Actb*) was used as internal control genes. The ΔΔCt method (Livak and Schmittgen, 2001) was used to calculate the relative mRNA expression. Data was accepted at < 40 cycles of amplification. Results are expressed as fold change to untreated control cultures maintained under normal medium conditions, set at 1 as baseline.

2.6. Sample preparation for proteomic analysis

Duplicate samples of control and 1 μM trimethyltin-treated cell pellets (immature and mature cultures, exposed to toxicant either 24 h or 10d) were solubilized in 6 M urea, 1 mM DTE, and 0.1 M TEAB. After homogenization steps, solubilized proteins were recovered by centrifugation in the supernatants.

Reduction of 10 μg of protein per sample was done with TCEP (tris (2-carboxyethyl)phosphine), final concentration of 10 mM, and samples reacted for 30 min at 30 °C. Alkylation was performed with iodoacetamide, added to a final concentration of 40 mM, and samples incubated 60 min in the dark at room temperature. Trypsin was added (ratio of 1:25, *w*/w), and the digestion was performed overnight at 37 °C. Then, a 10-plex Tandem mass tags (Thermo Scientific, Rockford, USA) labeling was performed according to manufacturer's instructions. Tandem mass tag reagents were dissolved in ACN, and each sample was incubated 60 min at room temperature with a specific tag. For tag quenching, 8 μL of hydroxylamin 5% (*V*/V) was added, and incubated with the samples for 15 min. Labeled samples were pooled and dried under vacuum. The sample was dissolved in 5% ACN/0.1% FA and desalted with C18 micro-spin columns (Thermo Scientific). Peptides were separated by off-gel electrophoresis (Geiser et al., 2011), desalted and solubilized in an appropriate amount of 5% ACN/0.1% FA for mass spectrometry (MS) analysis.

2.7. MS-data acquisition for proteomics analyses

For LC-MS/MS, peptides were dissolved in 5% ACN/0.1% FA to a concentration of 0.25 μg/μL. Mass spectrometry experiments were performed on a Q Exactive Plus instrument (Thermo Scientific, San Jose, CA, USA) equipped with an Easy-nanoLC (Thermo Scientific). Peptides were trapped on 2 cm × 75 μm ID, 3 μm pre-column and separated on an Easy-spray column, 50 cm × 75 μm ID, PepMap C18, 2 μm (Thermo Scientific). The analytical separation was run for 60 min using a gradient of 99.9% H_2O/0.1% (solvent A) and 99.9% ACN/0.1% FA (solvent B) at a flow rate of 300 nL min^{-1}. For MS survey scans, the OT resolution was set to 140,000 and the ion population was set to 3×10^6 with an *m/z* window from 350 to 2000. Twenty precursor ions were selected for higher-energy collisional dissociation (HCD) with a resolution of 35,000, an ion population set to 1×10^5 (isolation window of 0.5 *m/z*) and a normalized collision energy set to 30%.

2.8. Protein identification and quantification

Raw data were loaded on Proteome Discoverer 2.2 software for identification and/or quantification of peptides and proteins. Identification was performed in the UniProt/SwissProt (SwissProt rat database, containing 8039 entries) database using Mascot (Version 2.5.1, Matrix Sciences, London). Carbamidomethylation of cysteines, tandem mass tag - sixplex amino terminus and tandem mass tag - sixplex lysine (for labeled samples) were set as fixed modifications and methionine oxidation as variable modification. Trypsin was selected as the enzyme, with two potential miss-cleavages. Peptide and fragment ion tolerances were respectively 10 ppm and 0.02 Da. Threshold of the average reporter signal-to-noise ratio (S/N) was set to 2. False discovery ratio (FDR) was set to 1% at peptide-spectrum match (PSM), peptide and protein levels. Only high-confident master proteins with at least two distinct peptide sequences were required for identifications.

2.9. Pathway enrichment

Metacore v6.26 (Thomson Reuters) was used to analyze the significantly regulated proteins in the 4 groups compared resulting from the mass spectrometry analyses. Venny 2.1.0 was used to compare data sets (http://bioinfogp.cnb.csic.es/tools/venny/index.html).

2.10. Sample preparation and LC-MS analysis for metabolomics

Metabolomic analyses were performed on two different LC modes (reversed-phase LC –RPLC– and hydrophilic interaction LC –HILIC) in both positive and negative electrospray ionization polarities. Triplicate samples were used from every combination of the studied experimental factors: two maturation states (immature/mature), two exposure lengths (24 h or 10 days), and three trimethyltin doses (0.0, 0.5 and 1.0 μM). In order to stop the enzymatic activity and extract intracellular metabolites, 100 μL of ice-cold MeOH/H_2O (90:10, *v*/v) were added to each sample of neurospheres. Mechanical disruption was achieved by ultrasound treatment on ice (2 × 5 s) pulses, 30% amplitude, 2 mm-diameter probe operated on a VibraCell VCX 500 sonicator (Sonics & Materials Inc., Newtown, CT, USA). Samples were then centrifuged (12,000 × *g*, 15 mins, 4 °C) and supernatants collected. Aliquots of all cell extracts were pooled to generate a post-extraction quality control (QC) sample used for analytical performance evaluation and data treatment. Extracts were diluted 10 times prior to LC-MS analyses using either H_2O/MeCN (95:5, v/v) (for RPLC) or MeCN/H_2O (95, 5, v/v) (for HILIC).

Chromatography was performed on a Waters H-Class Acquity UHPLC system composed of a quaternary pump, a column manager, and a FTN auto sampler (Waters Corporation, Milford, MA, USA). For RPLC analyses, samples were separated on a Kinetex C18 column (150 × 2.1 mm, 1.7 μm) and the corresponding SecurityGuard Ultra precolumn and holder (Phenomenex, Torrance, USA). Solvent A was H_2O and solvent B was MeCN, both containing 0.1% FA. The column temperature and flow rate were set at 30 °C and 300 μL/min,

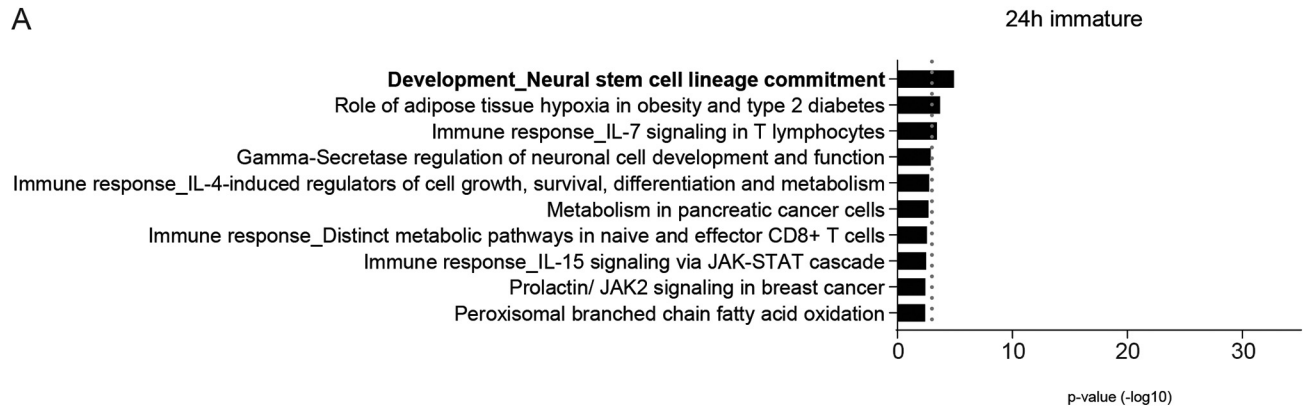

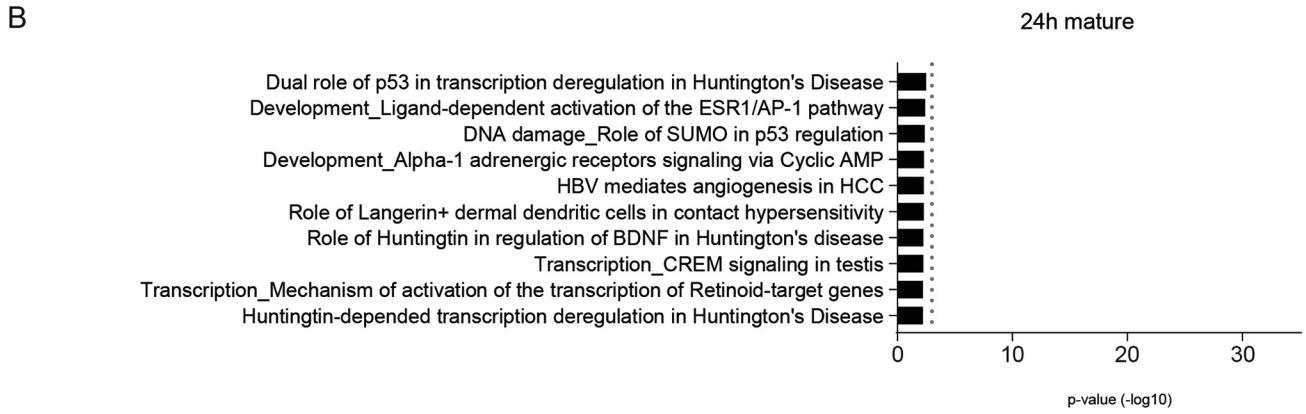

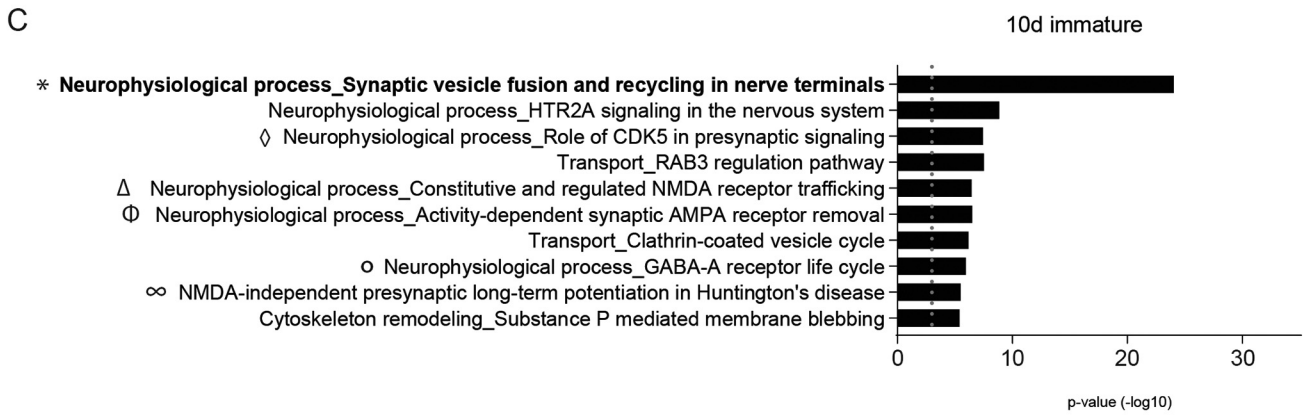

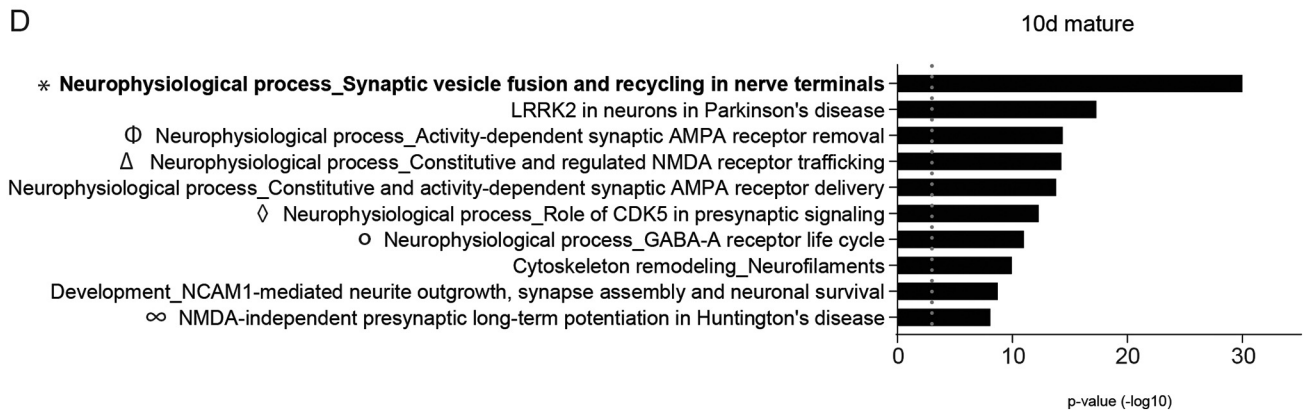

(caption on next page)

Fig. 2. Pathway analysis with MetaCore™. Proteins significantly up- or down-regulated (FC > 1.2, *p*-value < 0.05, *N* = 2 independent experiments each one resulting from a pool of 3 replicates) in immature cultures treated with TMT for 24 h (A), mature cultures treated with TMT for 24 h (B), immature cultures treated with TMT for 10 days (C) or mature cultures treated with TMT for 10 days (D), were selected to performed an enrichment of the biological pathways. The top 10 pathways for each condition are represented in the graph. X axis corresponds to (−log10) *p*-values, and a grey dash line represents the p-value cut-off at 0.001. Bold pathways are cited in the text, symbols represent identical pathways detected in immature and in mature cultures after the 10-d treatment.

respectively. The gradient elution was as follows: 2% to 100% B in 14 min, hold for 3 min, then back to 2% B in 0.1 min and re-equilibration of the column for 7.9 min. HILIC separations were conducted on a Waters Acquity BEH Amide column (150 × 2.1 mm, 1.7 µm) bearing a VanGuard pre-column. Solvent A was H_2O/MeCN (5:95, v/v) and solvent B was H_2O/MeCN (70:30, v/v) containing 10 mM ammonium formate (pH 6.5 in the aqueous part). The following gradient was applied: 0% B for 2 min, increased to 70% B over 18 min, held for 3 min, and then returned to 0% B to re-equilibrate the column for 7 min (total run time was 31 min). The flow rate was 500 µL/min, and the column temperature was kept at 40 °C. A sample volume of 5 µL was injected. Samples were randomized for injection, and QC pools were analyzed every 6 samples to monitor the performance of the analytical platform.

The UHPLC system was coupled to a maXis 3G Q-TOF high-resolution mass spectrometer (Bruker Daltonics GmbH, Bremen, Germany) through an electrospray interface (Gonzalez-Ruiz et al., 2018). The instrument was operated in TOF mode (no fragmentation). The capillary voltage was set at −4.7 kV for ESI+, drying gas temperature was 225 °C, drying gas flow rate was set at 5.50 (RPLC) or 8.00 (HILIC) L/min and nebulizing gas pressure was 1.8 (RPLC) or 2.0 bar (HILIC). Transfer time was set at 40 (RPLC) or 60 (HILIC) µs and prepulse storage time at 7.0 (Stenz et al., 2018) or 5.0 µs (HILIC). For ESI- operation, the capillary voltage was set at 2.8 kV. All the remaining ion source and ion optics parameters remained as in ESI+. Data between 50 and 1000 *m/z* were acquired in profile mode at a rate of 2 Hz. ESI and MS parameters were optimized using a mix of representative standards fed by a syringe pump and mixed with the LC eluent (mid-gradient conditions) within a tee-junction. Formate adducts in the *m/z* 90–1247 range were employed for in-run automatic calibration using the implemented quadratic plus high-precision calibration algorithm (Bruker). MS and UPLC control and data acquisition were performed through the HyStar v3.2 SR2 software (Bruker) running the Waters Acquity UPLC v.1.5 plug-in.

Run alignment, peak picking and sample normalization were performed on Progenesis QI v2.3 (Nonlinear Dynamics, Waters, Newcastle upon Tyne, UK) and peaks were identified by matching their retention times, accurate masses, and isotopic patterns to those of a library of chemical standards (MSMLS, Sigma-Aldrich, Buchs, Switzerland) analyzed under the same experimental conditions. Peaks were evaluated on the basis of the repeatability of their areas on the QC samples and discarded when the coefficient of variation was above 35% within the sequence.

2.11. Statistics

All obtained data were tested to be significantly different using 2-ways ANOVA test in conjunction with Tukey's multiple comparison test. *P*-values below 0.05 were considered as significant.

3. Results

3.1. TMT-exposed 3D rat brain model setting

Before performing proteomics and metabolomics analyses, TMT-induced neurotoxicity was evaluated in immature and differentiated 3D rat brain cell cultures treated either acutely, for 24 h, or repeatedly for 10 days with 0 (control), 0.5 or 1 µM of TMT from day *in vitro* (DIV) 5 to 15, or from DIV 25 to 35. TMT-induced cell death was assessed by measuring intracellular LDH activity and total protein content. The mRNA expression of *Hsp32* was analyzed as a marker of cellular stress associated to oxidative stress. Cell type-specific effects were evaluated by mRNA expression of *Nfh* (neurons), *Gfap* (astrocytes) and *Mbp* (oligodendrocytes).

No cytotoxicity was observed after the acute TMT treatment. In contrast, repeated exposure had a cytotoxic effect at the highest TMT concentration (1 µM), as shown by the significant decrease in both maturation stages of intracellular LDH activity (Fig. 1A).

Acute exposure did not affect the mRNA expression of *Hsp32*, while a concentration-dependent increase was found in immature and in differentiated cultures after the repeated treatment, pointing to cellular−/oxidative stress. No significant difference was found between immature and mature cultures (Fig. 1B).

All treatments caused neuronal cytoskeletal instability, as shown by the decrease of *Nfh* mRNA expression, indicating neurotoxic effects. The decrease was more pronounced in both immature and mature cultures after the repeated treatment than after acute exposure (Fig. 1C). Both in immature and mature cultures, repeated TMT treatment induced an upregulation of the astrocyte marker *Gfap* (Fig. 1D), a hallmark of astrocyte reactivity. However, no difference was found upon acute exposure at either maturation stage. Oligodendrocytes were not affected by the acute treatment, while repeated exposure caused a significant concentration-dependent decrease of *Mbp* expression specifically in immature cultures (Fig. 1E).

3.2. Protein changes associated to TMT exposure

To further elucidate TMT-induced neurotoxic mechanisms, and to decipher maturation-stage specific pathways involved in acute or repeated treatments, we used tandem mass tag technology to perform quantitative proteomics. Two independent experiments were conducted, comparing immature and mature cultures after 24 h and 10-day TMT exposure, respectively. A total of 2541 and 2422 proteins were identified (2 unique peptides, 1% FDR at the protein, peptide and PSM level) (supplementary Tables 1 and 2). Acute exposure caused a significant modification (up/down-regulation) of 55 proteins in immature cultures and of 17 in differentiated ones. While after 10-day repeated TMT exposure, 96 were modified in immature *versus* 353 in differentiated cultures. Among them, 69 proteins were affected in both differentiation stages, whereas 27 and 284 were exclusively modified in immature and in mature cultures, respectively (supplementary Tables 1 and 2).

3.3. Biological pathway modulation associated to TMT exposure

MetaCore curated databases allowed to perform a pathway enrichment analysis, based on the list of proteins showing modified expression, defined by the selected thresholds for the comparison of interest, *i.e.* fold change > 1.2 and *p*-value < 0.05.

In acutely exposed immature cultures, MetaCore identified the pathway linked to neural cell development called “Development – Neural stem cell lineage commitment”, (−log10(*p*-value) = 4.90), as the most relevant pathway with four specific proteins (GFAP, S100B, ATP1A2 and MCT1) (Fig. 2A, bold). No pathway was significantly highlighted after the single TMT treatment in mature cultures (Fig. 2B). Interestingly, in both immature and mature cultures exposed repeatedly to TMT, the most enriched pathway was “Synaptic vesicle fusion and recycling in nerve terminal” (Fig. 2C and D, bold), with 17 proteins among the 52 present in the pathways, showing altered regulation in

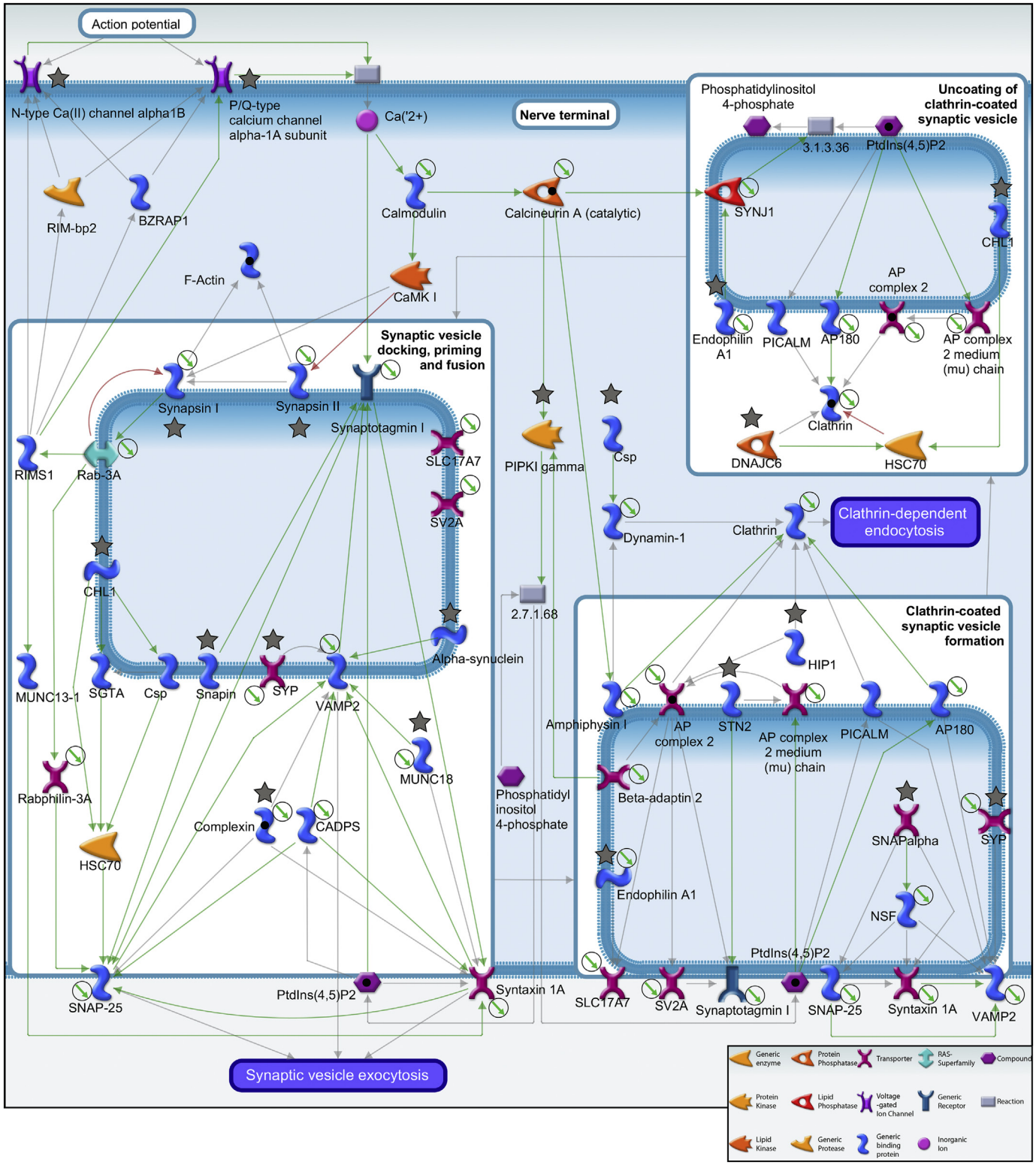

Fig. 3. Top biological pathway enriched in mature cell cultures exposed to TMT for 10 days. This neurophysiological process –"Synaptic vesicle fusion and recycling in nerve terminals"– has an enrichment *p*-value of 1.13×10^{-27}. A total of 27 proteins over the 52 represented in the pathways are modified by TMT treatment. Encircled green arrows indicate that protein was decreased in mature cell cultures exposed to TMT for 10 days in comparison to control. Grey stars represent secondary path start. Black dots on proteins means that it is a complex or a group of proteins. Long arrows connecting two proteins indicate a link between them, green is an activation, red an inhibition and grey means no effect or unspecified. (For interpretation of the references to colour in this figure legend, the reader is referred to the web version of this article.)

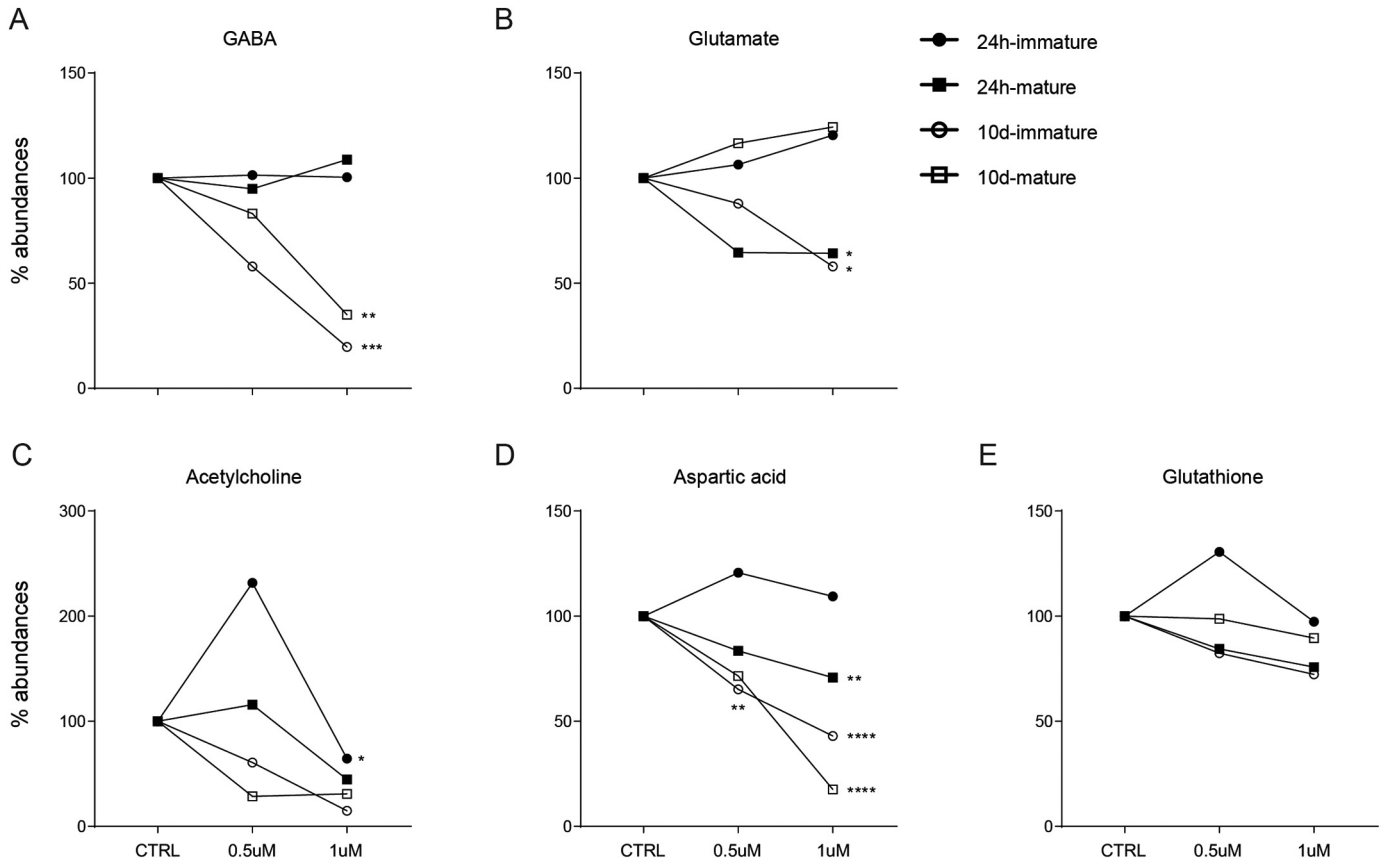

Fig. 4. Individual abundancies of 5 selected metabolites of interest. GABA (A), glutamate (B), acetylcholine (C), aspartic acid (D) and glutathione (E) normalized abundancies were plotted for each tested condition: immature and mature cultures, with 24 h and 10 days of TMT treatment ($N = 3$). Each dot is the result of the median of the three measures. Statistical significance of each measure from treated cells toward the control culture was assessed with a 2-ways ANOVA test in conjunction with Tukey's multiple comparison test. Significant p-values: * < 0.05; ** < 0.01; *** < 0.005; **** < 0.001.

immature cultures ($-\log10(p\text{-value}) = 21.2$), and 27 in mature cultures, reaching a highly significant enrichment p-value ($-\log10(p\text{-value}) = 29.9$). Additional pathways related to neurophysiological processes, neurotransmission mechanisms, synaptic communication, AMPA and NMDA physiology were also detected (Fig. 2D). As seen in details in Fig. 3, all proteins linked to the top enriched pathway were downregulated, indicating that sub-chronic TMT exposure perturbs vesicle transport and fusion. Calmodulin, which has a central role in this pathway, is downregulated together with Calcineurin. Both proteins represent the cornerstone in trafficking of synaptic vesicles pools. The observed decrease of Calmodulin impacts both Synapsin I and II levels, which are essential proteins for docking, priming and fusion of synaptic vesicles. Many proteins associated with these processes, such as Synapsin 1 and 2, Synaptotagmin-1, Vamp 2, SNAP-25 and nine others, are also down-regulated. Calmodulin is essential for the uncoating of clathrin-coated synaptic vesicles, a critical process for neurotransmitter release. As consequence of Calmodulin decrease is also the decrease of Calcineurin A, and directly of Endophilin A1, AP complex 2 and SYNJ1, which are involved in the filling of vesicles with neurotransmitters (Di Paolo et al., 2002; Sudhof, 2004; Sudhof and Rizo, 2011; Wu et al., 2009). A third group of affected proteins – Synaptophysin, Endophilin, SLC17A, Beta-adaptin and ten others – are related to clathrin-coated vesicle formation in synapses. The modulation of this group of proteins through Calmodulin, Calcineurin and Dynamin-1 down-regulation leads to perturbation of vesicle endocytosis.

TMT therefore impacts various synaptic vesicles processes, from vesicle formation, vesicles filling with neurotransmitters, to vesicle trafficking and exocytosis.

Raw data of each pathway enrichment analysis are presented in supplemental Table 3.

3.4. Proteins of interest related to cell type-specific effects and to mechanisms of toxicity

Proteins of interest related to cell-type specific effects and to already known TMT mechanisms of toxicity, as well as results previously obtained in 3D rat brain cell cultures, were extracted from the lists. All detailed information on protein ratios are found in supplemental Tables 1 and 2.

3.4.1. Cell type specific effects

Effects on neurons were analyzed by considering changes of proteins of the cytoskeleton and of proteins related to specific neurotransmitters. Regarding neuronal processes and specific neuronal subtypes, no significant change was found after acute TMT treatment. In contrast, the repeated exposure caused a significant decrease of two of the three neurofilament proteins (medium and low) molecular weight (NF-M and NF-L), which were both significantly decreased in mature cultures. Other cytoskeletal elements, such as MAP2, tau, as well as the enzyme neuron specific enolase (NSE) were similarly decreased following the repeated TMT treatment (see supplementary material, protein list). The glutamic acid decarboxylase (GAD), an enzyme specific of GABAergic neurons was significantly decreased in immature cultures after repeated TMT treatment. A marker of glutamatergic neurotransmission, VGlut1, was affected in mature cultures after repeated TMT exposure. Regarding the vesicular and synaptic machinery, as highlighted by the pathway enrichment analysis, a great number of

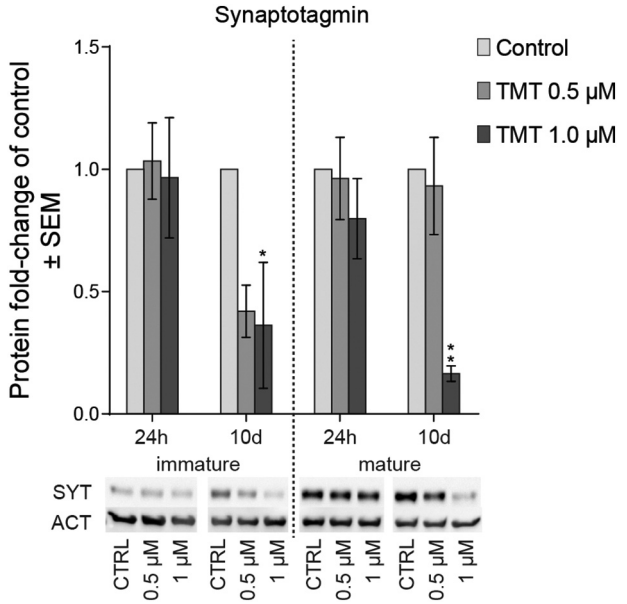

Fig. 5. Western blot analyses of synaptotagmin-1 (SYT), as verification of proteomic data, were conducted on immature and mature 3D rat brain cell cultures exposed to 0.5 µM and 1 µM of TMT for 24 h or 10 days. Quantification of actin (ACT) level was used for normalization. The bars correspond to the standard error of the mean (SEM) of band volumes with the standard deviation (N = 3). Statistical significance of each measure from treated cells toward the control culture was assessed with a 2-ways ANOVA test in conjunction with Tukey's multiple comparison test. Significant *p*-values: * < 0.05; ** < 0.01; *** < 0.005; **** < 0.001.

involved proteins were modified. No significant change was observed following acute exposure at either maturation stages, whereas the repeated treatment caused a decreased expression of these proteins, which tended to be more pronounced in differentiated cultures than in the immature.

Two specific astrocytic proteins, protein S100−B and aquaporin 4, were significantly decreased in immature cultures after acute TMT treatment, while no significant change was observed in differentiated cultures. The repeated treatment caused an upregulation of GFAP in mature cultures. In addition, in mature cultures, proteins localized in astrocytes or linked to neuroinflammatory processes – such as Galectin 3 or Annexin A1 – were significantly upregulated.

3.4.2. Effects related to oxidative stress

In analogy to the observations made on mRNA level (Fig. 1), HSP 32 also called heme oxygenase-1 (HO-1) was upregulated in both immature and differentiated cultures exclusively after the repeated treatment. Interestingly, glutathione peroxidase (GPx), involved in detoxification of reactive oxygen radicals (ROS), showed a similar pattern of modification as HO-1. Other proteins involved in protection against oxidative stress, such as the metallothioneins-1 and -2, (MT1, MT2), were upregulated in both maturation stages, but exclusively after repeated TMT treatment.

3.5. Metabolomic analysis and immunoblotting for validation of proteomic analysis

A metabolomic approach was applied to reveal metabolites, in particular neurotransmitter levels, which may be altered as a consequence of vesicle trafficking impairment observed in the proteomics pathway analysis. While GABA levels were decreased in both maturation stages only after the 10-day treatment (Fig. 4A), glutamate content showed a different pattern; significantly decreasing after the acute treatment in mature cultures, and in immature cultures after the 10-day treatment (Fig. 4B). Acetylcholine levels were not significantly modified in any situation (Fig. 4C). Aspartic acid content was significantly affected in all situations, except in the immature cultures exposed acutely to TMT (Fig. 4D). Finally, no significant change was found in any condition for glutathione levels (Fig. 4E), the main molecule involved in oxidative stress protection. Raw data for these 5 metabolites are presented in supplemental Table 4.

Western blot analysis was used to assess Synaptotagmin-1 expression, associated to the enriched pathways “Synaptic vesicle fusion and recycling in nerve terminals” and “Role of CDK5 in presynaptic signalling” both enriched in immature and mature cultures with repeated TMT treatment. No effect was detected after acute exposure in both maturation stages, but a significant decrease of Synaptotagmin expression was observed in 3D cultures submitted to repeated TMT treatment. This effect was more pronounced in immature cultures, where it was visible also at the lower TMT concentration (0.5 µM) (Fig. 5).

4. Discussion

The mechanisms of TMT-induced toxicity involving oxidative stress, excitotoxicity and neuroinflammation have mainly been studied *in vivo*, in adult animals, where TMT injection is reported to induce neurodegeneration in the hippocampus (Corvino et al., 2013; Little et al., 2012; Geloso et al., 2011; Fiedorowicz et al., 2001; Chang, 1990; Shintani et al., 2007; Tang et al., 2013). The present study was performed *in vitro* using 3D rat brain cell cultures, where decrease of intracellular LDH activity and protein content indicated neural cell death after repeated treatment to 1 µM TMT. However, 24 h after a single TMT treatment, no significant cell death was detected, but proteomic profiling allowed to detect alterations of biological pathways, which may give information about the early events of TMT's mode of action in neural tissues, or about potential adaptive mechanisms.

Brain development is a vulnerable window for xenobiotic exposure (Grandjean and Landrigan, 2014), with specific neurodevelopmental events exhibiting particular susceptibility (Aschner et al., 2017; Bal-Price et al., 2015). Previous studies using 3D cultures of rat telencephalon showed a higher sensitivity of the immature brain cells to TMT treatment (Monnet-Tschudi et al., 1995a). By considering a broad number of proteins associated with different neural cell types and cellular compartments, proteomic pathway analysis allowed a more precise analysis of TMT-induced effects in immature and differentiated brain cells, shedding light on development-dependent effects. Interestingly, acute TMT treatment induced alterations in a greater number of pathways in immature cultures compared to the mature. However, the reverse scenario was observed following the repeated treatment, indicating that immature cultures have a stronger response to an acute exposure, whereas differentiated cultures respond stronger to a prolonged exposure. Since the differentiation process leads to an increased expression and abundance of proteins possibly affecting the detection level, this potential bias has been corrected for by normalization of total protein content.

In immature brain cell cultures the main pathway affected by TMT acute exposure, according to the pathway analysis performed in this study, was “Development_Neural stem cell lineage commitment”. Interestingly, three of the four modified proteins are specific of astrocytes, suggesting that astrocyte maturation may be an important target of TMT-induced adverse effects. However, gene expression suggests that neurons are also very sensitive to TMT treatment as seen by a strong decrease in *Nfh* mRNA expression already after 24 h exposure in both stages. Metacore pathway analysis also revealed that the ATPase subunit 1A2 (ATP1A2) was also affected by acute exposure of immature cultures. ATP1A2 is predominantly expressed in neurons in neonates and in astrocytes in adult, where it modulates the reuptake of potassium and glutamate from the synaptic cleft (Kinoshita et al., 2016). Determination of the primary target of TMT exposure turned out to be

difficult, as it may be concealed by the progressive differentiation-dependent changes as well as by the various cell populations and their interactions.

The main pathway highly affected after the repeated TMT treatment in both maturation stages was “Synaptic vesicle fusion and recycling in nerve terminals”, with 17 proteins and 27 proteins in immature and in mature cultures, respectively out of the 52 described in the biological pathway. Proteins involved in synaptic vesicle formation, as well as in synaptic vesicle docking, priming and fusion were downregulated, suggesting that TMT strongly affects neurotransmitter release. Although this pathway was altered in both immature and differentiated cultures, the consequences may be different. During development, neurotransmitter release has trophic effects on the maturation of target neurons and such disturbances may directly affect network formation (Mirmiran and Swaab, 1986). Studies have shown that GABA, which is a predominant inhibitory neurotransmitter that regulates glutamatergic activity and is involved in synaptic plasticity (Kim et al., 2015) in adult brain, is an excitatory neurotransmitter in the immature brain. Furthermore, during development it acts as a trophic factor and is involved in the establishment of higher brain functions, such as memory and learning (Takayama and Inoue, 2004). This is of particular relevance for this study, since the main neurotransmitter system affected by TMT treatment is GABA, as evidenced by the significant decrease of GAD in both developmental stages. A developmental comparison of TMT effects on GABA neurotransmission between juvenile (postnatal day 24) and adult rats (postnatal day 56) showed complex and dynamic regulation of GABA receptor subunits mRNA level and GABA-related protein expression during postnatal development and following TMT exposure, with a more pronounced neurodegeneration in juvenile animals (Kim et al., 2015). In adult brain, Nishimura and colleagues observed, in contrast to the present results, an increase in GAD-65 mRNA level in hippocampus of adult rats five days after TMT dosage (Nishimura et al., 2001). Baciak and colleagues, on the other hand, did not evidence any change in GABA content as a consequence of TMT-induced neurodegeneration, whereas fish exposed to TMT showed an increase of GABA content (Baciak et al., 2017; Zuo et al., 2009). Brodie and colleagues observed an increase of GABA level in hippocampus of rats 48 h post TMT exposure, followed by a decrease at 72 h post-exposure, when necrotic changes were well established (Brodie et al., 1990). Taken together these observations suggest dynamic changes in GABA neurotransmission following TMT exposure, with initial upregulation as adaptive response, followed by a decrease at a later stage of TMT exposure.

In addition to perturbations of GABAergic neurotransmission, metabolomic analysis revealed a decrease of glutamate content in immature cultures after acute exposure and in mature cultures after the 10-d TMT treatment, as well as concomitant decreased VGlut1 expression in mature cultures (data not shown), firmly points to an altered glutamatergic neurotransmission. This corroborates previous observations *in vivo* showing a decrease of glutamate in hippocampus, while glutamine level was increased (Baciak et al., 2017). Interestingly, Baciak et al., also described a decrease of *N*-acetylaspartate. In accordance, metabolomic investigations revealed a decrease of aspartic acid at both maturation stages after the repeated TMT treatment, as well as in acutely treated mature cultures. A previous report by Mailman and co-workers (Mailman et al., 1983) on the effects of TMT on several neurotransmitters systems in different brain areas showed that, in contrast to GABA and glutamate, acetylcholine level was not affected in any brain area, while dopamine concentration was decreased in striatum, but neither in brainstem, nor in cerebellum. The present results obtained in 3D cultures prepared from whole brain of rat embryos and containing the different neuronal subtypes revealed no significant alterations in acetylcholine (Fig. 4C) and dopamine and its precursor L-tyrosine levels (data not shown).

TMT treatment also triggers other cellular responses. The upregulation of *Hsp32* mRNA and protein expression, as well as an upregulation of GPx, detected after the 10-day treatment in both immature and mature cultures suggest that the neurotoxic insult is coupled with a prominent oxidative stress. No development-dependent differences were observed regarding oxidative stress, in contrast with a previous report showing that immature cultures are more sensitive to repeated paraquat exposure than mature ones, due to development-dependent perturbation of glutathione-mediated defence mechanism (Sandstrom et al., 2017). As TMT-induced oxidative stress seems to be associated to the neurodegenerative process, it could be secondary to glial cell reactivity, underlying the neuroinflammatory process (Hsieh and Yang, 2013).

The association of neuroinflammation with TMT-induced neurodegeneration has widely been described (Bruccoleri et al., 1998; Harry et al., 2008; Harry and Lefebvre d'Hellencourt, 2003; Harry et al., 2002; Little et al., 2002; Monnet-Tschudi et al., 1995b). Indeed, repeated TMT treatment resulted in the upregulation of GFAP, a marker of astrocyte reactivity, in both immature and differentiated cultures. In differentiated cultures also other markers of astrocyte reactivity, such as vimentin, S-100, as well of other more general markers of neuroinflammation, such as the galectins and annexins (McArthur et al., 2010; Sirko et al., 2015) showed increased expression. The neuroinflammatory process seems to be more pronounced in differentiated cultures than in the immature. Similar effects have previously been reported in 3D rat brain cell aggregates exposed to the herbicide paraquat, where immature cultures showed a limited neuroinflammatory response of a less protective phenotype (Sandstrom et al., 2017). Interestingly, the astrocytic specific protein aquaporin 4 was upregulated at both stages after repeated TMT treatment, as well as in differentiated cultures after acute exposure. A recent study suggests that aquaporin 4 may be involved in synaptic plasticity (Szu and Binder, 2016). Metacore pathway analysis indicated strong effects on the synaptic machinery in immature cultures – hence during synapse formation – and in differentiated cultures - during synaptic stabilization – suggesting that the upregulation of aquaporin 4 may be part of an adaptive mechanism.

In conclusion, proteomic profiling, metabolomics approaches and pathway analysis suggested that the vesicular and synaptic machinery of GABA and glutamate neurotransmission were the most affected by TMT exposure, with strong alterations upon repeated exposure when the neurodegenerative process is ongoing. Comparison of effects in immature and differentiated neural cells revealed the difficulty of evidencing development-dependent differences, due to the duration of the insult or due to the progressive differentiation process itself. Considering the mechanisms of TMT neurotoxicity – oxidative stress and synaptic neurodegeneration – no significant differentiation-dependent differences could be observed, while neuroinflammation appeared to be more pronounced in differentiated cultures. However, pathway analysis revealed that specific developmental events, such as neural stem cells lineage commitment, were perturbed in immature cultures following acute TMT treatment. Acute TMT treatment also perturbed astrocyte and oligodendrocyte markers, which are still differentiating in immature cultures, as previously described (Zurich et al., 2004). A previous study by Schultz and coworkers (Schultz et al., 2015) has shown that the 3D brain cell culture system in a differentiated stage is well suited for OMIC's analysis after both acute and prolonged treatments. The present study extends this application for potential comparison of developmental neurotoxicity testing (DNT) and aspects of neurotoxicity testing (NT). Furthermore, the association of proteomic and metabolomic techniques using pathway analysis provides a toolset for a more holistic comparison of perturbed pathways at different stages of exposure and duration of xenobiotic insult.

Supplementary data to this article can be found online at https://doi.org/10.1016/j.tiv.2019.05.020.

Acknowledgments

We are grateful to the Swiss Centre for Applied Human Toxicology for funding this study. We also want to thank Alexandre Hainard, Carla Pasquarello and Patrizia Arboit from the proteomic core facility of the Geneva University for their kind help and advices for the proteomic analyses by mass spectrometry. Alexandra Broyer and Denise Tavel are greatly acknowledged for their technical assistance in the maintenance and treatments of the 3D rat brain cell cultures and for performing the immunoblots.

References

Agency for Toxic Substances and Disease Registry (ATSDR), 2005. Toxicological Profile for Tin. U.S. Department of Health and Human Services, Public Health Service, Atlanta, GA.

Andersson, H., Radesater, A.C., Luthman, J., 1995. Trimethyltin-induced loss of NMDA and kainate receptors in the rat brain. Amino Acids 8 (1), 23–35.

Aschner, M., et al., 2017. Reference compounds for alternative test methods to indicate developmental neurotoxicity (DNT) potential of chemicals: example lists and criteria for their selection and use. ALTEX 34 (1), 49–74.

Baciak, L., et al., 2017. In vivo magnetic resonance approach to trimethyltin induced neurodegeneration in rats. Brain Res. 1673, 111–116.

Bal-Price, A., et al., 2015. Putative adverse outcome pathways relevant to neurotoxicity. Crit. Rev. Toxicol. 45 (1), 83–91.

Brambilla, P., et al., 2003. GABAergic dysfunction in mood disorders. Mol. Psychiatry 8 (8), 721–737, 715.

Brodie, M.E., et al., 1990. Neurochemical changes in hippocampal and caudate dialysates associated with early trimethyltin neurotoxicity in rats. Neurotoxicology 11 (1), 35–46.

Bruccoleri, A., Brown, H., Harry, G.J., 1998. Cellular localization and temporal elevation of tumor necrosis factor-alpha, interleukin-1 alpha, and transforming growth factor-beta 1 mRNA in hippocampal injury response induced by trimethyltin. J. Neurochem. 71 (4), 1577–1587.

Chang, L.W., 1990. The neurotoxicology and pathology of organomercury, organolead, and organotin. J. Toxicol. Sci. 15 (Suppl. 4), 125–151.

Corvino, V., et al., 2013. Neuroprotective strategies in hippocampal neurodegeneration induced by the neurotoxicant trimethyltin. Neurochem. Res. 38 (2), 240–253.

Di Paolo, G., et al., 2002. Decreased synaptic vesicle recycling efficiency and cognitive deficits in amphiphysin 1 knockout mice. Neuron 33 (5), 789–804.

Fiedorowicz, A., et al., 2001. Dentate granule neuron apoptosis and glia activation in murine hippocampus induced by trimethyltin exposure. Brain Res. 912 (2), 116–127.

Geiser, L., et al., 2011. Shotgun proteomics: a relative quantitative approach using off-gel electrophoresis and LC-MS/MS. Methods Mol. Biol. 681, 459–472.

Geloso, M.C., Corvino, V., Michetti, F., 2011. Trimethyltin-induced hippocampal degeneration as a tool to investigate neurodegenerative processes. Neurochem. Int. 58 (7), 729–738.

Gonzalez-Ruiz, V., et al., 2018 May. ROMANCE: a new software tool to improve data robustness and feature identification in CE-MS metabolomics. Electrophoresis 39 (9-10), 1222–1232. https://doi.org/10.1002/elps.201700427.

Grandjean, P., Landrigan, P.J., 2014. Neurobehavioural effects of developmental toxicity. Lancet Neurol. 13 (3), 330–338.

Harry, G.J., Lefebvre d'Hellencourt, C., 2003. Dentate gyrus: alterations that occur with hippocampal injury. Neurotoxicology 24 (3), 343–356.

Harry, G.J., et al., 2002. Morphological alterations and elevations in tumor necrosis factor-alpha, interleukin (IL)-1alpha, and IL-6 in mixed glia cultures following exposure to trimethyltin: modulation by proinflammatory cytokine recombinant proteins and neutralizing antibodies. Toxicol. Appl. Pharmacol. 180 (3), 205–218.

Harry, G.J., et al., 2008. The type 1 interleukin 1 receptor is not required for the death of murine hippocampal dentate granule cells and microglia activation. Brain Res. 1194, 8–20.

Hogberg, H.T., et al., 2009. Gene expression as a sensitive endpoint to evaluate cell differentiation and maturation of the developing central nervous system in primary cultures of rat cerebellar granule cells (CGCs) exposed to pesticides. Toxicol. Appl. Pharmacol. 235 (3), 268–286.

Honegger, P., Lenoir, D., Favrod, P., 1979. Growth and differentiation of aggregating fetal brain cells in a serum-free defined medium. Nature 282 (5736), 305–308.

Honegger, P., et al., 2011. Preparation, maintenance, and use of serum-free aggregating brain cell cultures. Methods Mol. Biol. 758, 81–97.

Hsieh, H.L., Yang, C.M., 2013. Role of redox signaling in neuroinflammation and neurodegenerative diseases. Biomed. Res. Int. 2013, 484613.

Kim, J., et al., 2014. Glial activation with concurrent up-regulation of inflammatory mediators in trimethyltin-induced neurotoxicity in mice. Acta Histochem. 116 (8), 1490–1500.

Kim, J., et al., 2015. Developmental and degenerative modulation of GABAergic transmission in the mouse hippocampus. Int. J. Dev. Neurosci. 47 (Pt B), 320–332.

Kinoshita, P.F., et al., 2016. The influence of Na(+), K(+)-ATPase on glutamate signaling in neurodegenerative diseases and senescence. Front. Physiol. 7, 195.

Koh, J.Y., Choi, D.W., 1987. Quantitative determination of glutamate mediated cortical neuronal injury in cell culture by lactate dehydrogenase efflux assay. J. Neurosci. Methods 20 (1), 83–90.

Lee, S., et al., 2016. Trimethyltin-induced hippocampal neurodegeneration: a mechanism-based review. Brain Res. Bull. 125, 187–199.

Little, A.R., et al., 2002. Chemically induced neuronal damage and gliosis: enhanced expression of the proinflammatory chemokine, monocyte chemoattractant protein (MCP)-1, without a corresponding increase in proinflammatory cytokines(1). Neuroscience 115 (1), 307–320.

Little, A.R., et al., 2012. Trimethyltin-induced neurotoxicity: gene expression pathway analysis, q-RT-PCR and immunoblotting reveal early effects associated with hippocampal damage and gliosis. Neurotoxicol. Teratol. 34 (1), 72–82.

Livak, K.J., Schmittgen, T.D., 2001. Analysis of relative gene expression data using real-time quantitative PCR and the 2(−Delta Delta C(T)) method. Methods 25 (4), 402–408.

Lowry, O.H., et al., 1951. Protein measurement with the Folin phenol reagent. J. Biol. Chem. 193 (1), 265–275.

Mailman, R.B., et al., 1983. Effects of postnatal trimethyltin or triethyltin treatment on CNS catecholamine, GABA, and acetylcholine systems in the rat. J. Neurochem. 40 (5), 1423–1429.

McArthur, S., et al., 2010. Annexin A1: a central player in the anti-inflammatory and neuroprotective role of microglia. J. Immunol. 185 (10), 6317–6328.

McCann, M.J., et al., 1996. Differential activation of microglia and astrocytes following trimethyl tin-induced neurodegeneration. Neuroscience 72 (1), 273–281.

Mirmiran, M., Swaab, D.F., 1986. Central neurotransmitter disturbances underlying developmental neurotoxicological effects. Neurotoxicology 7 (2), 95–102.

Monnet-Tschudi, F., et al., 1995a. Effects of trimethyltin (TMT) on glial and neuronal cells in aggregate cultures: dependence on the developmental stage. NeuroToxicology 16, 97–104.

Monnet-Tschudi, F., et al., 1995b. Microglial responsiveness as a sensitive marker for trimethyltin (TMT) neurotoxicity. Brain Res. 690 (1), 8–14.

Monnet-Tschudi, F., Zurich, M.G., Honegger, P., 1996. Comparison of the developmental effects of two mercury compounds on glial cells and neurons in aggregate cultures of rat telencephalon. Brain Res. 741 (1–2), 52–59.

Nemes, P., et al., 2013. Qualitative and quantitative metabolomic investigation of single neurons by capillary electrophoresis electrospray ionization mass spectrometry. Nat. Protoc. 8 (4), 783–799.

Nicholson, J.K., Lindon, J.C., Holmes, E., 1999. 'Metabonomics': understanding the metabolic responses of living systems to pathophysiological stimuli via multivariate statistical analysis of biological NMR spectroscopic data. Xenobiotica 29 (11), 1181–1189.

Nicholson, J.K., et al., 2002. Metabonomics: a platform for studying drug toxicity and gene function. Nat. Rev. Drug Discov. 1 (2), 153–161.

Nishimura, T., et al., 2001. Changes in the GABA-ergic system induced by trimethyltin application in the rat. Brain Res. Mol. Brain Res. 97 (1), 1–6.

Pottiez, G., et al., 2011. A differential proteomic approach identifies structural and functional components that contribute to the differentiation of brain capillary endothelial cells. J. Proteome 75 (2), 628–641.

Sandstrom, J., et al., 2017. Potential mechanisms of development-dependent adverse effects of the herbicide paraquat in 3D rat brain cell cultures. Neurotoxicology 60, 116–124.

Schultz, L., et al., 2015 Dec 25. Evaluation of drug-induced neurotoxicity based on metabolomics, proteomics and electrical activity measurments in complementary CNS in vitro models. Toxicol. in Vitro 30 (1 Pt A), 138–165. https://doi.org/10.1016/j.tiv.2015.05.016.

Shin, E.J., et al., 2016. Protein kinase Cdelta mediates trimethyltin-induced neurotoxicity in mice in vivo via inhibition of glutathione defense mechanism. Arch. Toxicol. 90 (4), 937–953.

Shintani, N., et al., 2007. Recent studies on the trimethyltin actions in central nervous systems. Yakugaku Zasshi 127 (3), 451–461.

Sirko, S., et al., 2015. Astrocyte reactivity after brain injury-: the role of galectins 1 and 3. Glia 63 (12), 2340–2361.

Stenz, L., et al., 2018. Intergenerational transmission of DNA methylation signatures associated with early life stress. Curr. Genomics 19 (8), 665–675.

Sudhof, T.C., 2004. The synaptic vesicle cycle. Annu. Rev. Neurosci. 27, 509–547.

Sudhof, T.C., Rizo, J., 2011. Synaptic vesicle exocytosis. Cold Spring Harb. Perspect. Biol. 3 (12).

Szu, J.I., Binder, D.K., 2016. The role of astrocytic aquaporin-4 in synaptic plasticity and learning and memory. Front. Integr. Neurosci. 10, 8.

Takayama, C., Inoue, Y., 2004. GABAergic signaling in the developing cerebellum. Anat. Sci. Int. 79 (3), 124–136.

Tang, X., et al., 2013. Toxicity of trimethyltin and dimethyltin in rats and mice. Bull. Environ. Contam. Toxicol. 90 (5), 626–633.

Teismann, P., Schulz, J.B., 2004. Cellular pathology of Parkinson's disease: astrocytes, microglia and inflammation. Cell Tissue Res. 318 (1), 149–161.

van Vliet, E., et al., 2008. A novel in vitro metabolomics approach for neurotoxicity testing, proof of principle for methyl mercury chloride and caffeine. Neurotoxicology 29 (1), 1–12.

Wilmes, A., et al., 2013. Application of integrated transcriptomic, proteomic and metabolomic profiling for the delineation of mechanisms of drug induced cell stress. J. Proteome 79, 180–194.

Wong, C.G., Bottiglieri, T., Snead 3rd, O.C., 2003. GABA, gamma-hydroxybutyric acid, and neurological disease. Ann. Neurol. 54 (Suppl. 6), S3–S12.

Wu, X.S., et al., 2009. Ca(2+) and calmodulin initiate all forms of endocytosis during depolarization at a nerve terminal. Nat. Neurosci. 12 (8), 1003–1010.

Yoo, C.I., et al., 2007. A case of acute organotin poisoning. J. Occup. Health 49 (4), 305–310.

Zuo, Z., et al., 2009. Acute administration of tributyltin and trimethyltin modulate glutamate and N-methyl-D-aspartate receptor signaling pathway in Sebastiscus marmoratus. Aquat. Toxicol. 92 (1), 44–49.

Zurich, M.-G., et al., 2002. Maturation-dependent neurotoxicity of lead aceate in vitro: implication of glial reactions. J. Neurosci. Res. 70, 108–116.
Zurich, M.-G., et al., 2003. Aggregating brain cell cultures for neurotoxicological studies. In: Tiffany-Castiglioni, E. (Ed.), In vitro Neurotoxicology: Principles and Challenges. Humana Press Inc., Totowa, NJ, pp. 243–266.
Zurich, M.G., et al., 2004. Involvement of glial cells in the neurotoxicity of parathion and chlorpyrifos. Toxicol. Appl. Pharmacol. 201 (2), 97–104.